Lattice dynamics in the *ab*- and *bc*-spiral spin-ordered states of perovskite manganites

J. S. Lee,[1,*] N. Kida,[1] Y. Yamasaki,[2] R. Shimano,[1,3] and Y. Tokura[1,2,4]

[1]*Multiferroics Project, Exploratory Research for Advanced Technology (ERATO), Japan Science and Technology Agency (JST), c/o Department of Applied Physics, University of Tokyo, Tokyo 113-8656, Japan*

[2]*Department of Applied Physics, University of Tokyo, Tokyo 113-8656, Japan*

[3]*Department of Physics, The University of Tokyo, Tokyo 113-0033, Japan*

[4]*Cross-Correlated Materials Research Group (CMRG), ASI, RIKEN, Wako, Saitama 351-0198, Japan*

(Received 19 July 2009; revised manuscript received 15 September 2009; published 8 October 2009)

We have investigated infrared lattice dynamics in the multiferroic states of $Gd_{1-x}Tb_xMnO_3$ (x=0.3 and 0.5) to explore the coupling between the optical phonons and the electromagnons, the latter of which are characteristic collective excitations in the spiral spin-ordered (ferroelectric) state. Upon magnetic transitions, most of the phonon modes exhibit strong variations in their peak positions and/or spectral weights. Among them, three low-frequency phonons polarized along the a axis are found to show a strong coupling with the electromagnons. The sum rule indicates that these modes are mainly responsible for the electric dipole activity of the electromagnons via their mutual coupling.

DOI: 10.1103/PhysRevB.80.134409 PACS number(s): 78.30.−j, 76.50.+g, 75.80.+q, 75.47.Lx

Recently, multiferroelectricity has been attracting great interest for its possible applications exploiting magnetoelectric phenomena.[1–3] For the multiferroic perovskite manganites, the spontaneous polarization (P_S) is produced by the spiral spin order, and can be flopped by changing the spiral spin plane with an application of the magnetic field;[4,5] the direction of P_S can be changed from the c axis to the a axis by applying the magnetic field along the b axis. The coupling between the spiral spin order and the electric polarization can be well explained by the inverse Dzyaloshinskii-Moriya interaction,[6–8] as expressed by $P_S \propto e_{ij} \times (S_i \times S_j)$, where e_{ij} is the unit vector connecting spin moments S_i and S_j at sites i and j.

Another important magnetoelectric phenomenon for the perovskite manganites is the appearance of electromagnons (EM),[9–19] magnetic excitations driven by an electric field (E) component of light. While the EM appears mainly in the spiral spin-ordered state as the spontaneous polarization does, it is hardly affected by the change in the spiral spin plane. Irrespective of the direction of spiral planes, two distinct EM excitations are observed only along the a axis,[11–19] as revealed by, for example, the detailed study of $DyMnO_3$ in magnetic fields.[12] In this context, the origin of the EM has recently been attributed to the Heisenberg interaction,[16,17,19,20] which can induce the symmetric spin-dependent electric dipole (p_{sym}) as $p_{sym} \propto \Pi_{ij}(S_i \cdot S_j)$, where Π_{ij} is the local electric dipole formed between S_i and S_j. Although this mechanism cannot produce a net polarization in the static state for the perovskite manganites, it can generate a coherent induction of local dipole moments in response to $E \| a$ which accompanies an excitation of the zone-edge magnon. In this way, both the light polarization dependence and the characteristic energies of the EM located around 60 cm^{-1} could be well explained.

To deepen the understanding of such a newly found excitation, its possible coupling to the other excitations, such as the phonons and/or the electronic transitions, should be clarified. In particular, the problem how the electric-dipole activity of the EM arises is important to solve experimentally in the light of the spin-orbit coupling and spin-lattice interaction in multiferroics. Upon the magnetic transition to the spiral spin-ordered state, the lowest-lying phonon mode exhibits large changes in its peak position and spectral weight (SW), which have been regarded as signatures of the coupling between the EM and the phonon.[10,11,15,19] On the other hand, even if all the SW, which the lowest-lying phonon is losing, would be transferred to the EM, it is responsible for only part of the SW of the EM, typically 30–50 %. While Valdés Aguilar *et al.*[11] have argued that the sum rule may be almost conserved by including contributions from all the phonons, it is not clear how the SW transfer occurs for each phonon mode.

In this paper, we investigate a complete set of optical phonons polarized along all the three crystallographic axes for multiferroic perovskite manganites exploring the coupling between phonons and the EM. For this purpose, we focus on the $Gd_{0.7}Tb_{0.3}MnO_3$ compound since it has versatile magnetic/electric phases as a function of temperature (T).[21] In particular, it shows an abrupt transition from the ferroelectric/spiral spin-ordered state to the paraelectric/A-type antiferromagnetic (A-AFM) state as temperature decreases through $T_{A\text{-}AFM} \sim 14$ K. This phase transition accompanies a complete suppression of the EM abruptly from its maximum response,[14,17] which provides a unique opportunity to examine how the phonons are influenced by the existence or disappearance of the EM. We monitored the energy position and the SW of phonons upon temperature-dependent magnetic transitions. From the comparison among the behaviors of all the phonons along each crystallographic axis, we demonstrate that the phonons along the a axis are much more strongly coupled to the magnetic system and the three $E \| a$ lower-lying modes are mainly responsible for the electric-dipole activity of the EM.

Single crystals of $Gd_{1-x}Tb_xMnO_3$ (x=0.3 and 0.5) were grown by a floating zone method.[22] As temperature decreases, both compounds undergo the transitions, first from the paramagnetic to the collinear spin-ordered state around 42 K, and then to the ferroelectric/spiral spin-ordered state around 24 K. Each compound has different directions of P_S and the spiral plane: $P_S \| c$ in the bc spiral state for the

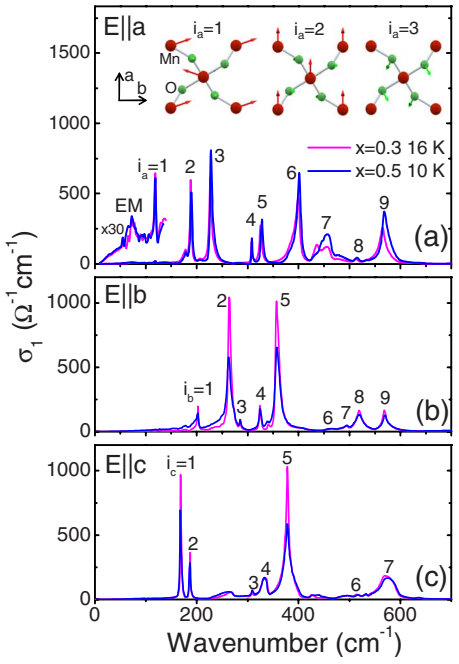

FIG. 1. (Color online) The optical conductivity spectra $\sigma_1(\omega)$ below 700 cm^{-1} at 16 K for $Gd_{0.7}Tb_{0.3}MnO_3$ and at 10 K for $Gd_{0.5}Tb_{0.5}MnO_3$ along (a) the *a* axis, (b) the *b* axis, and (c) the *c* axis. In (a), the spectra below 150 cm^{-1} are multiplied by 30. The insets of (a) shows the displacements of Mn and O ions for the modes i_a=1, 2, and 3 referring to Ref. 24.

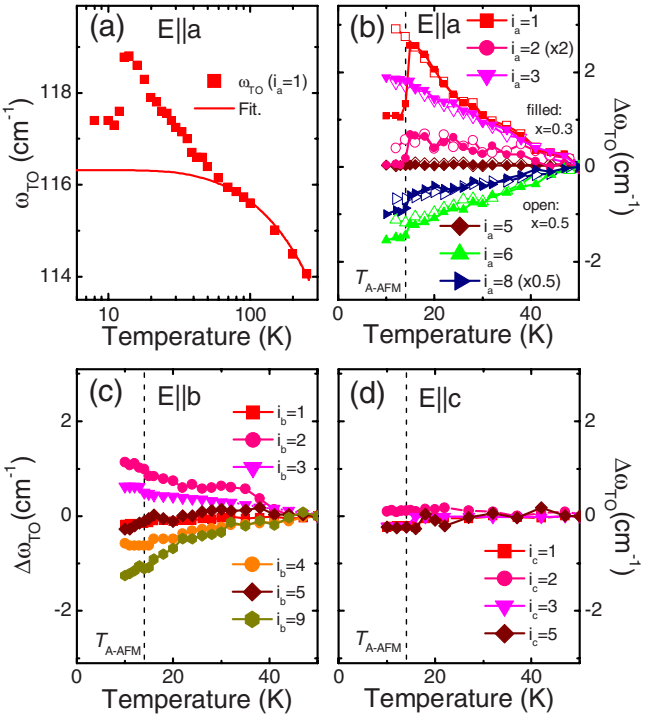

FIG. 2. (Color online) (a) Temperature-dependent peak positions of the lowest-lying phonon (i_a=1) polarized along the *a* axis. Solid line corresponds to the model calculation based on the anharmonic thermal effect (see text). [(b)–(d)] Temperature-dependent peak positions of representative phonon modes polarized along the *a*, *b*, and *c* axes. The values ($\Delta\omega_{TO}$) at each temperature correspond to the phonon frequency shifts from the frequency at 50 K.

x=0.5 compound and $P_S \| a$ in the *ab* spiral state for the x =0.3 compound. As noted above, the x=0.3 compound experiences an additional transition to the paraelectric/A-AFM state around 14 K. We measured temperature-dependent reflectivity spectra above 40 cm^{-1} using Fourier-transform spectroscopy, and determined complex optical constants through the Kramers-Kronig transformation. For the extrapolation of the reflectivity below 40 cm^{-1}, we used the optical constants obtained by terahertz time-domain spectroscopy.[17]

Figure 1 shows the real part of the optical conductivity spectra, $\sigma_1(\omega)$, below 700 cm^{-1} at 16 K for the x=0.3 compound and at 10 K for the x=0.5 compound. For $E \| a$, $\sigma_1(\omega)$ multiplied by 30 are also shown below 150 cm^{-1}, where well-defined peak structures are discernible at about 75 and 120 cm^{-1} for both compounds. While the latter one is the lowest-lying optical phonon, the former one corresponds to the zone-edge EM, which is in good agreement with previous results obtained from a transmission (and reflectivity) measurement of the thin sample.[17] Incidentally, the lower-lying EM around 20 cm^{-1} is not well discernible in these spectra. It should be noted that while each compound has different spiral planes, they show similar EM excitations confirming that the EMs originate from the symmetric spin interaction as mentioned above.

Besides these low-intensity excitations for $E \| a$, there are several sharp peaks observed in the far-infrared region with the light electric field along each crystallographic axis. For the orthorhombic perovskite, a group-theoretical analysis for *Pbnm* space group shows that there are 25 infrared-active zone-center phonons, such as $7B_{1u}$(*c*-axis)$+9B_{2u}$(*b*-axis) $+9B_{3u}$(*a*-axis).[23,24] The number of the phonons along each axis roughly agrees with such a prediction. Nevertheless, there are a few more peak structures observed than those expected, which may be due to a slight misorientation of the sample and hence a finite contribution of phonons along the other directions. In this work, we discuss the phonons with a clear peak structure as marked with the numbers on the corresponding peaks.

To investigate lattice dynamics in relation to magnetic orders, especially to the spiral spin-order accompanying the emergence of the well-defined EM, we first examine temperature-dependent variations in the peak position of each phonon. In Fig. 2(a), we show, as an example, the phonon frequency ω_{TO} for the $E \| a$ lowest-lying mode, i.e., the mode i_a=1 in a full temperature range investigated. As temperature decreases, ω_{TO} shows a gradual increase and then a much steeper increase below about 50 K at which the spin order sets in. With further decreasing temperature, ω_{TO} shows the maximum in the ferroelectric/spiral spin-ordered state at about 14 K, and then a sudden drop upon the transition to the A-AFM state. With a conventional temperature effect alone, the phonon frequency would increase with decreasing temperature and become saturated below about 50 K as shown with a solid line in Fig. 2(a), following the relation that $\omega_{TO}(T)=\omega_{TO}^0-\alpha[2/(e^{\omega_{TO}/2k_BT}-1)+1]$.[25] Here, ω_{TO}^0 is an eigenfrequency of the phonon, k_B is the Boltzmann constant, and α is a constant. For the curve in Fig. 2(a), ω_{TO}^0=116.8 cm^{-1} and α=0.48 cm^{-1} were used. Therefore, a

deviation of the peak position from such conventional lattice anharmonicity can be attributed to coupling of the lattice to the other degree of freedom; this is the magnetic order in the present case.

Figures 2(b)–2(d) show the frequency shifts $\Delta\omega_{TO}(T)$ of several representative phonons for $E\|a$, b, and c, respectively, with respect to the values at 50 K, i.e., $\Delta\omega_{TO}(T) = \omega_{TO}(T) - \omega_{TO}$ (50 K). For the $E\|a$ phonons, while three lower-lying modes (i_a=1–3) show blueshifts, three higher-lying modes (i_a=6–8) show redshifts, and two intermediate modes (i_a=4 and 5) located in between and the highest frequency mode i_a=9 exhibit almost no discernible frequency shift within our experimental accuracy. (The results for i_a =4, 7, and 9 are not shown.) Around 14 K when the x=0.3 compound enters the A-AFM state, most of the phonons which have shown finite frequency shifts in the spiral spin-ordered state undergo additional anomalies. This clearly indicates that such behaviors of phonon frequencies originate from the coupling of phonons with the spin degree of freedom. For the $E\|b$ phonons, while their frequencies also exhibit finite temperature dependence, the changes are less than for the $E\|a$ phonons. For the $E\|c$ phonons, most of the modes show little temperature dependence. This suggests that the lattice dynamics along the a axis is more strongly coupled to the magnetic system than along the other axes. Note that the x=0.3 and 0.5 compounds exhibit almost the same behaviors in the phonon frequencies [Fig. 2(b)] except for some additional anomalies upon entering the A-AFM state below 14 K for the x=0.3 compound. Considering that each compound has different spiral spin-order planes, i.e., *ab* and *bc* planes for the x=0.3 and 0.5 compounds, respectively,[21] it is likely that the symmetric spin exchange interaction determines such behaviors of the phonon frequency.

For the phonons involved with dynamic displacements of magnetic ions, modulations of exchange energies by the lattice vibration can shift their frequencies; $\Delta\omega_{TO}^{sp} = \lambda\langle S_i \cdot S_j\rangle$.[26–29] Here, λ is a coupling constant proportional to the second derivative of the exchange energies with respect to atomic displacements of the phonon, and $\langle S_i \cdot S_j\rangle$ represents the averaged spin correlation between the sites i and j. In a given magnetic state, each mode should have different coupling strengths depending on the modulation strength of the exchange energies by the vibration of the corresponding mode.

In the A-AFM state, the spin correlations for all the bonds connecting Mn ions are equally given as $|\langle S_i \cdot S_j\rangle| \approx 4$. Then the effective spin-phonon coupling strength $|\lambda_{eff}|$, which includes modulations of all the relevant exchange energies by the corresponding phonon mode, can be estimated. For instance, modes i_a=1, 3, and 6 have the effective coupling constants $|\lambda_{eff}| \sim 0.3$, 0.5, and 0.4, respectively. Note that these values are comparable to those of other antiferromagnetic compounds.[26–29]

To discuss the possible coupling between the phonons and the EM, we pay attention to anomalies of the phonon frequencies at $T_{\mathrm{A-AFM}}$. As noted above, additional anomalies of the phonon frequency upon the spiral to A-AFM transition can give a clue to spin-phonon coupling relevant to the EM. The nearest-neighbor spin correlation $|\langle S_i \cdot S_j\rangle|/4$ in the *ab* plane changes from 0.71 in the spiral spin-ordered state (a spin modulation vector q_m=0.256) to 1 in the A-AFM state.[21] Provided that exchange energies between nearest neighbors in the *ab* plane are mainly involved in the spin-phonon coupling for $E\|a$ and $E\|b$ phonons,[30] the frequency shift in the A-AFM state would be larger in its amplitude than the value in the spiral spin-ordered state while keeping the same sign. As shown in Figs. 2(b) and 2(c), such behaviors can be found for most of the modes, such as i_a=6 and 8, and i_b=2, 3, 4, and 9. On the other hand, the frequency shifts for the modes i_a=1, 2, and 3 strongly deviate from such behaviors. As temperature decreases, the frequency shift of the mode i_a=1 increases to about 2.5 cm^{-1} in the spiral spin-ordered state, but it becomes smaller to have about 1 cm^{-1} in the A-AFM state. Similar behaviors can be found for the mode i_a=2 while the absolute values of the change are much smaller. For the mode i_a=3, while the frequency increases by about 2.0 cm^{-1} in the spiral spin-ordered state, it experiences almost no change upon the A-AFM transition.

A plausible origin for these anomalous behaviors is the coupling of phonons with the EM. Provided the coupling between the EM and the phonon, the frequency of the phonon tends to blueshift in the presence of the EM in the spiral spin-ordered state.[31,32] Then upon the transition from the spiral spin-ordered state to the A-AFM state, the frequency shift of the phonons located in the low-frequency region should be determined by a competition of two factors: (i) the simple spin-phonon coupling shifting the frequency further in the same direction as in the spiral spin-ordered state, i.e., the further blueshift for three low-frequency modes (i_a=1–3); and (ii) the disappearance of the EM-phonon coupling shifting the phonons to the lower frequency. When the latter effect is dominant, the phonon frequency should become smaller in the A-AFM state, which is the case for i_a=1 and 2. When both effects are comparable, the frequency would not apparently change, which corresponds to the case for i_a=3. In both cases, the behaviors of the phonon frequency deviating from the prediction based on the simple spin-phonon coupling can be attributed to the coupling between the EM and the corresponding phonon modes.

Let us now discuss the behaviors of the SW of the phonons. The SW of each mode was estimated by integrating $\sigma_1(\omega)$; $\mathrm{SW}(T) = \int_{\omega_1}^{\omega_2} \sigma_1(\omega) d\omega$, and $\Delta\mathrm{SW}(T) = \mathrm{SW}(T) - \mathrm{SW}(50\ \mathrm{K})$. Here, the both-end cut-off frequencies for the integration were chosen as the frequencies around where $\sigma_1(\omega)$ has a local minimum between the phonon peaks. This estimation was performed also for the EM. The values for the EM and the lowest-lying phonon agree well with those reported earlier,[11,15,17] which proves the validity of this analysis. For the x=0.3 compound, as temperature decreases from 50 K down to 15 K, SW of the EM increases by 1.0×10^4 cm^{-2} [Fig. 3(a)]. In the A-AFM state below 14 K, it becomes almost zero confirming that the EM is active mainly in the spiral spin-ordered state. In accord with such spectral changes in the EM, the lowest-lying phonon shows noticeable spectral changes; its SW continues to decrease with decreasing temperature down to 15 K, and recovers back in the A-AFM state. It should be noted that such a behavior is completely opposite to that of the EM, which provides a direct evidence of the strong coupling between the EM and

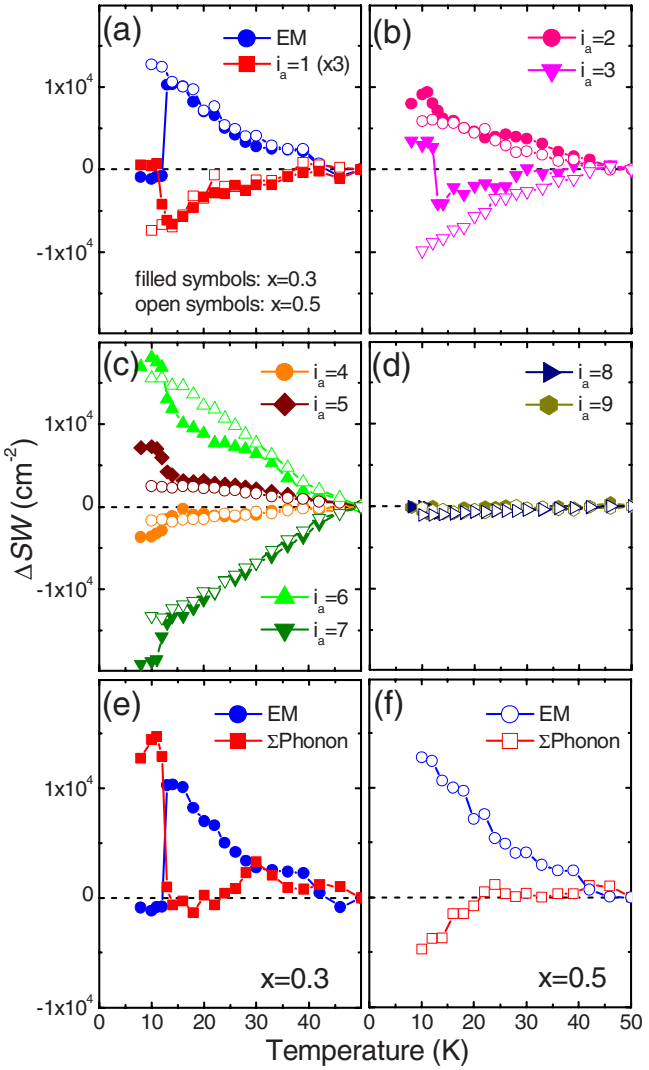

FIG. 3. (Color online) Temperature-dependent spectral weights for the phonons polarized along the a axis for $Gd_{0.7}Tb_{0.3}MnO_3$ (filled symbols) and for $Gd_{0.5}Tb_{0.5}MnO_3$ (open symbols). The values correspond to the differences between the SW at 16 and 50 K. (a) The results for the mode i_a=1. The values for the EM are also shown. The results for the modes (b) i_a=2 and 3, (c) i_a=4–7, and (d) i_a=8 and 9. (e) and (f): the sum of ΔSW for all the phonons (ΣPhonon) and the ΔSW of the electromagnon for the x=0.3 compound and x=0.5 compound, respectively.

this phonon mode. Importantly, however, the absolute value of the SW change in the phonon is much smaller than that of the EM. To satisfy the optical sum rule, it is clear that the higher energy contribution, either/both from the other phonons or/and from the electronic excitations, should be included.

Figures 3(b)–3(d) show the temperature-dependent changes in the SWs for the other phonon modes. Interestingly, most of the modes, except for the modes i_a=8 and 9, show much larger SW changes than the lowest-lying mode. In particular, ΔSW's of modes i_a=6 and 7 even exceed that of EM. Two modes located next to each other, i.e., the modes i_a=4 and 5, and the modes i_a=6 and 7 are showing opposite temperature dependences. Therefore, the net change in the respective pair modes appears small. Such an antisymmetric behavior for the neighboring mode pair is less pronounced for the low-frequency modes, i.e., modes i_a=1–3.

For the perovskite transition metal oxides, as the crystal symmetry lowers from the cubic to the orthorhombic one, phonons split and mix with each other. Upon the magnetic transition, structural symmetry can be affected through a finite magnetoelastic coupling which can modify the hybridization between neighboring modes and lead to the spectral-weight redistribution between them as observed. Details of the spectral-weight transfer, such as direction and magnitude of the respective spectral-weight transfer, would depend on the symmetry of relevant phonons and their relations to the magnetic system, of which discussion is beyond the scope of the present work.

In Figs. 3(e) and 3(f), the sum of the spectral weights of all the phonons are shown for the x=0.3 and 0.5 compound, respectively. Here, the spectral contribution between 130 and 160 cm^{-1} was excluded where the excitation related to the Tb ion appears.[33] For the both compounds, the phonon SW decreases in the spiral spin-ordered state. In the A-AFM state for the x=0.3 compound, it increases by about 1.5 $\times 10^4$ cm^{-2}. In the same figure, the SW change in the EM is also shown. Overall, the T dependence of the SW of EM is opposite to that of the net SW of all the phonons. Nevertheless, the total summation of them seems to be bigger than zero with respect to the value at 50 K, indicating that the SW sum rule is not fully satisfied in this frequency region. This may be due to a finite contribution of the thermal effect in this temperature range and/or a change in the kinetic energy of the electronic system upon the magnetic transitions.

In order to minimize thermal effects and to focus on the influence of the EM on spectral changes in the phonons, we monitored differences of SWs (δSW) for the x=0.3 compound at 16 and 12 K when EM has the maximum and minimum responses, respectively. In Figs. 4(a)–4(c), the δSW values of the respective modes are displayed at their frequency positions at 50 K. Upon the transition between the A-AFM and spiral spin-ordered state, SWs of the $E\|a$ phonons show noticeable changes and the summation of δSW for all the phonons amounts to about -1.5×10^4 cm^{-2}. The $E\|b$ and $E\|c$ phonons also exhibit finite changes in SW, but their net contributions are much smaller than for the $E\|a$ phonons: $\sim0.3\times10^4$ cm^{-2} for $E\|b$ and $\sim0.4\times10^4$ cm^{-2} for $E\|c$.

Such a large reduction in the SW for the $E\|a$ phonons can be attributed to the transfer of their SW to the EM. The SW for the EM was estimated to be about 1.2×10^4 cm^{-2}. Then the total sum including the EM and all the phonons, both polarized along the a axis, is about -0.3×10^4 cm^{-2}. Note that the magnitude of this value is quite comparable to the values along the other axes. Such finite amounts of spectral-weight changes in the terahertz/far-infrared region cannot be due to the thermal effect; it may be related to the change in a kinetic energy of the electronic system upon the magnetic transition. This consideration leads us to conclude that the optical sum rule related to the emergence/disappearance of the EM is almost satisfied by including the contribution of the phonons.

It should be noted that three $E\|a$ lower-lying modes are

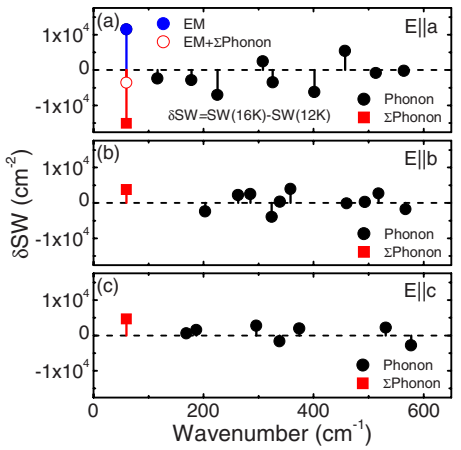

FIG. 4. (Color online) The spectral-weight changes (δSW) upon the transition from the A-AFM state (12 K) to the spiral spin-ordered state (16 K) for the phonon modes polarized along (a) the *a* axis, (b) the *b* axis, and (c) the *c* axis. The values are displayed at the frequency of the corresponding modes at 50 K. The values for the EM is shown at 70 cm^{-1}. The total contribution of all the phonons (ΣPhonon) and its summation with the EM contribution are also shown at the same frequency.

mainly responsible for this sum rule satisfaction; while the higher-lying modes i_a=4–7 also exhibit spectral changes, their contributions are compensated by neighboring modes. As discussed above, signatures of the coupling between the EM and these phonons were found also in the temperature-dependent changes in mode frequencies. For the perovskite manganites, the $E\|a$ phonons modulate the exchange energies along the *b* axis by the coherent modulation of the bond length and bond angle as shown in the inset of Fig. 1(a) for i_a=1–3. This then couples to the excitation of the zone-edge magnon,[16,17] and the spectral-weight transfer from the phonon to the EM can be expected. While such a coupling mechanism can be valid for all the phonons polarized along the *a* axis, the larger energy separation for the higher-lying phonons would reduce the coupling strength and should be responsible for their less contribution to the electric-dipole activity of the EM.

Finally, it is worth to discuss the lattice dynamics in relation to the ferroelectric ordering. For the perovskite manganites, ferroelectricity arises with $P_S\|c$ in the *bc*-spiral spin-ordered state and $P_S\|a$ in the *ab*-spiral spin-ordered state, which corresponds to the cases of the x=0.5 and 0.3 compounds, respectively. If the ferroelectricity would be involved with the displacement of the ions along the polarization direction,[34] the infrared phonons polarized along the same direction should undergo some anomalies, for instance, a frequency softening of relevant phonon modes, and such behaviors should be discriminated depending on the directions of the spontaneous polarization. As shown above, however, we could not find any meaningful difference in the infrared lattice dynamics between the x=0.5 and 0.3 compounds.[35] This suggests either that the ferroelectricity of these compounds is not strongly coupled to the lattice degree of freedom, or that such a coupling results in lattice distortions smaller than our experimental accuracy. This is totally consistent with a recent observation on the absence of anomaly of the *c*-polarized phonon dispersion in the similar *bc*-spiral state of $TbMnO_3$.[36]

In summary, we have discussed the lattice dynamics of the perovskite manganites $Gd_{1-x}Tb_xMnO_3$ (x=0.3 and 0.5) focusing on their possible couplings to the electromagnon. Upon magnetic transitions, while most of the phonon modes exhibit strong anomalies in their peak positions and/or spectral weights, the three $E\|a$ lower-lying modes show clear signatures of the coupling with the electromagnon. In particular, they are found to be fully responsible for the electric dipole activity of the electromagnon. Although the other $E\|a$ phonons also would have similar matrix elements of the coupling with the electromagnon, the larger energy separation between the electromagnon and these modes should reduce the coupling strength drastically.

We thank M. Mochizuki, T. Arima, and N. Nagaosa for fruitful discussion. This work was in part supported by Grant-in-Aids for Scientific Research (Grants No. 16076205 and No. 20340086) from the Ministry of Education, Culture, Sports and Technology (MEXT), Japan.

*jslee@erato-mf.t.u-tokyo.ac.jp

[1] T. Kimura, T. Goto, H. Shintani, K. Ishizaka, T. Arima, and Y. Tokura, Nature (London) **426**, 55 (2003).
[2] Y. Tokura, Science **312**, 1481 (2006).
[3] S.-W. Cheong and M. Mostovoy, Nature Mater. **6**, 13 (2007).
[4] T. Kimura, G. Lawes, T. Goto, Y. Tokura, and A. P. Ramirez, Phys. Rev. B **71**, 224425 (2005).
[5] N. Abe, K. Taniguchi, S. Ohtani, T. Takenobu, Y. Iwasa, and T. Arima, Phys. Rev. Lett. **99**, 227206 (2007).
[6] H. Katsura, N. Nagaosa, and A. V. Balatsky, Phys. Rev. Lett. **95**, 057205 (2005).
[7] I. A. Sergienko and E. Dagotto, Phys. Rev. B **73**, 094434 (2006).
[8] M. Mostovoy, Phys. Rev. Lett. **96**, 067601 (2006).
[9] A. Pimenov, A. A. Mukhin, V. Yu. Ivanov, V. D. Travkin, A. M. Balbashov, and A. Loidl, Nat. Phys. **2**, 97 (2006).
[10] A. Pimenov, T. Rudolf, F. Mayr, A. Loidl, A. A. Mukhin, and A. M. Balbashov, Phys. Rev. B **74**, 100403(R) (2006).
[11] R. Valdés Aguilar, A. B. Sushkov, C. L. Zhang, Y. J. Choi, S. W. Cheong, and H. D. Drew, Phys. Rev. B **76**, 060404(R) (2007).
[12] N. Kida, Y. Ikebe, Y. Takahashi, J. P. He, Y. Kaneko, Y. Yamasaki, R. Shimano, T. Arima, N. Nagaosa, and Y. Tokura, Phys. Rev. B **78**, 104414 (2008).
[13] A. Pimenov, A. Loidl, A. A. Mukhin, V. D. Travkin, V. Yu. Ivanov, and A. M. Balbashov, Phys. Rev. B **77**, 014438 (2008).
[14] N. Kida, Y. Yamasaki, R. Shimano, T. Arima, and Y. Tokura, J. Phys. Soc. Jpn. **77**, 123704 (2008).
[15] Y. Takahashi, N. Kida, Y. Yamasaki, J. Fujioka, T. Arima, R. Shimano, S. Miyahara, M. Mochizuki, N. Furukawa, and

Y. Tokura, Phys. Rev. Lett. **101**, 187201 (2008).
[16] R. Valdés Aguilar, M. Mostovoy, A. B. Sushkov, C. L. Zhang, Y. J. Choi, S.-W. Cheong, and H. D. Drew, Phys. Rev. Lett. **102**, 047203 (2009).
[17] J. S. Lee, N. Kida, S. Miyahara, Y. Takahashi, Y. Yamasaki, R. Shimano, N. Furukawa, and Y. Tokura, Phys. Rev. B **79**, 180403(R) (2009).
[18] N. Kida, Y. Takahashi, J. S. Lee, R. Shimano, Y. Yamasaki, Y. Kaneko, S. Miyahara, N. Furukawa, T. Arima, and Y. Tokura, J. Opt. Soc. Am. B **26**, A35 (2009).
[19] Y. Takahashi, Y. Yamasaki, N. Kida, Y. Kaneko, T. Arima, R. Shimano, and Y. Tokura, Phys. Rev. B **79**, 214431 (2009).
[20] S. Miyahara and N. Furukawa, arXiv:0811.4082 (unpublished).
[21] Y. Yamasaki, H. Sagayama, N. Abe, T. Arima, K. Sasai, M. Matsuura, K. Hirota, D. Okuyama, Y. Noda, and Y. Tokura, Phys. Rev. Lett. **101**, 097204 (2008).
[22] T. Goto, Y. Yamasaki, H. Watanabe, T. Kimura, and Y. Tokura, Phys. Rev. B **72**, 220403(R) (2005).
[23] I. S. Smirnova, Physica B (Amsterdam) **262**, 247 (1999).
[24] N. N. Kovaleva, A. V. Boris, L. Capogna, J. L. Gavartin, P. Popovich, P. Yordanov, A. Maljuk, A. M. Stoneham, and B. Keimer, Phys. Rev. B **79**, 045114 (2009).
[25] J. Menendez and M. Cardona, Phys. Rev. B **29**, 2051 (1984), and references therin.
[26] K. Wakamura, Solid State Commun. **71**, 1033 (1989).
[27] J. Laverdière, S. Jandl, A. A. Mukhin, V. Yu. Ivanov, V. G. Ivanov, and M. N. Iliev, Phys. Rev. B **73**, 214301 (2006).
[28] T. Rudolf, Ch. Kant, F. Mayr, J. Hemberger, V. Tsurkan, and A. Loidl, Phys. Rev. B **76**, 174307 (2007).
[29] J. S. Lee, T. W. Noh, J. S. Bae, In-Sang Yang, T. Takeda, and R. Kanno, Phys. Rev. B **69**, 214428 (2004).
[30] A contribution from the next-nearest-neighboring exchange energies is considered as a secondary effect since the infrared active phonons involve no modulation of the oxygen-oxygen bond mediating next-nearest-neighboring Mn ions. A possible contribution from Tb ions is not included since the long-range order of their spin moments occurs below about 7 K (Ref. 4).
[31] H. Katsura, A. V. Balatsky, and N. Nagaosa, Phys. Rev. Lett. **98**, 027203 (2007).
[32] T. Yildirim, L. I. Vergara, Jorge Íñiguez, J. L. Musfeldt, A. B. Harris, N. Rogado, R. J. Cava, F. Yen, R. P. Chaudhury, and B. Lorenz, J. Phys.: Condens. Matter **20**, 434214 (2008).
[33] As reported in Refs. 15 and 17, the excitation related to the Tb ion is located around 135 cm^{-1} just above the lowest-lying phonon for $E\|a$. While the spectral weight of this mode is comparable to that of the lowest-lying phonon, it shows little change upon the transition to the A-AFM state (Ref. 17). Therefore, this contribution can be excluded when discussing the spectral weight of the EM which is completely suppressed in the A-AFM state.
[34] H. J. Xiang, Su-Huai Wei, M.-H. Whangbo, and Juarez L. F. Da Silva, Phys. Rev. Lett. **101**, 037209 (2008); A. Malashevich and D. Vanderbilt, *ibid.* **101**, 037210 (2008).
[35] While the spectral-weight changes for $i_a=3$ and 7 (Fig. 3) exhibit finite differences between the $x=0.3$ and 0.5 compounds, their possible connection to the ferroelectricity is not clear at the present stage.
[36] R. Kajimoto, H. Sagayama, K. Sasai, T. Fukuda, S. Tsutsui, T. Arima, K. Hirota, Y. Mitsui, H. Yoshizawa, A. Q. R. Baron, Y. Yamasaki, and Y. Tokura, Phys. Rev. Lett. **102**, 247602 (2009).